P2.20

Classification of precipitation types during transitional winter weather using the RUC model and polarimetric radar retrievals

H.- S. Park[1], A. Ryzhkov[2], H. Reeves[2], and T. Schuur[2]

[1]*Department of Astronomy and Atmospheric Sciences, Kyungpook National University, Daegu, South Korea*

[2]*Cooperative Institute for Mesoscale Meteorological Studies, Oklahoma University and NOAA/OAR National Severe Storms Laboratory, Norman Oklahoma*

1. Introduction

The ability of dual-polarization radar to distinguish between precipitation types offers great potential for improving nowcasting capabilities for winter storms. The operational version of the hydrometeor classification algorithm (HCA) accepted for the polarimetric WSR-88D, however, was primarily developed for warm season weather and has been mainly tested on summer-type storms. There is therefore a need to modify and generalize the existing classification routine to better address classification issues related to transitional winter weather, such as the detection of freezing rain, and discrimination between rain, ice pellets / sleet, and different types of snow.

To improve the HCA, we must first recognize shortcoming of existing classification techniques. First, as noted above, the existing HCA was primarily developed for warm season weather. Classification of ice phase precipitation often requires an accurate estimation of the melting level height through detection of the radar bright band (Giangrande et al. 2008). Because of this, it may not work efficiently for cold-season storms for which the height of melting layer (if it exists at all) is below 1 km. Second, it is essentially "local". That is, it provides class designations at every elevation sweep, only using radar information collected at that sweep rather than in a full 3D volume of radar data. Because of this, precipitation type is determined only from data observed on conical surfaces and does not necessarily represent hydrometeor types near the ground. Third, and perhaps most importantly, the existing polarimetric HCA is entirely radar-based; no thermodynamic information is utilized in the classification process.

In this study, an experimental version of a winter precipitation classifier that uses thermodynamic information derived from a numerical prediction model is developed and tested for a high-impact storm that occurred over central Oklahoma on 30 November 2006. The storm produced a sequence of convective rain, freezing rain, and ice pellets, followed by wet and dry snow with variable density.

2. Classes and input variables

The classification algorithm described in this paper distinguishes between 9 classes of precipitation *near the surface*. As noted above, this is distinctly different than the existing version of the algorithm which, at the lowest WSR-88D scanning elevation of 0.5°, provides a classification based on observations collected several kilometers *above the surface* at distant ranges from the radar. The technique presented here combines data collected from the polarimetric KOUN WSR-88D radar, located in Norman, Oklahoma, with thermodynamic data obtained from a numerical prediction model. The winter precipitation classes provided by this algorithm, which is described in detail in the following sections, are:

Corresponding author address:
Alexander V. Ryzhkov, CIMMS/NSSL, 120 David L. Boren Drive, Norman, OK 73072.
Email: Alexander.Ryzhkov@noaa.gov

(1) Crystals (CR)
(2) Dry snow (DS)
(3) Wet snow (WS)
(4) Ice pellets / sleet (IP)
(5) Freezing rain (FR)
(6) Freezing rain and ice pellets mix (FR/IP)
(7) Rain (RA)
(8) Heavy rain (HR)
(9) Hail (HA)

The suite of polarimetric variables used as input is the same as for existing the existing HCA: Z, Z_{DR}, K_{DP}, ρ_{hv}, SD(Z), and SD(Φ_{DP}). Ryzhkov et al. (2005) and Park et al. (2009) provide a detailed description of polarimetric data processing and classification, respectively. Required thermodynamic information used as input includes vertical profiles of temperature T, dewpoint temperature T_d, and pressure p with the spatial resolution, which is available from existing NWP models. A prototype version of the algorithm is tested using the Rapid-Update-Cycle (RUC) model analyses which have a horizontal grid spacing of 20 km and a vertical grid distance of 25 hPa starting at 1000 hPa and extending to 100 hPa. These analyses are created by blending the 1-hr forecast from the previous forecast cycle with available observations from surface, upper-air, aircraft, and satellite and radar data. The RUC analyses are provided every hour.

3. Storm description

The event in question is caused by a strong northeast-to-southwest oriented cold front that moved eastward across Oklahoma on 30 November 2006. A snapshot of the RUC-analyzed 2-m temperature 0000 UTC 30 November 2006 shows the leading edge of the front is over southeast Oklahoma. There are subfreezing temperatures over central and western Oklahoma at this time. A time sequence of vertical profiles of wet bulb temperature (T_w) at Kessler Farm Field Laboratory (KFFL, location is provided in Fig. 1) shows there is an elevated warm layer between about 1 and 3 km above ground from 0000 to 1300 UTC (Fig. 2). As the front moves further eastward, the elevated warm layer is removed so that by 1500 UTC, the entire vertical profile has temperatures that are less than 0°C.

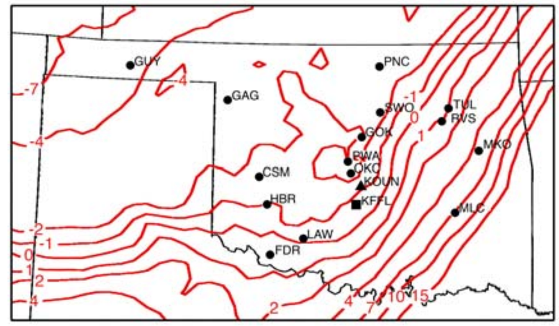

Fig. 1: The RUC-analyzed 2-m temperature (contoured). Locations of select NWS surface observation stations are included (marked with closed circles) as is the KOUN surface observation, upper-air, and radar location (triangle) and the disdrometer at Kessler Farm (closed square).

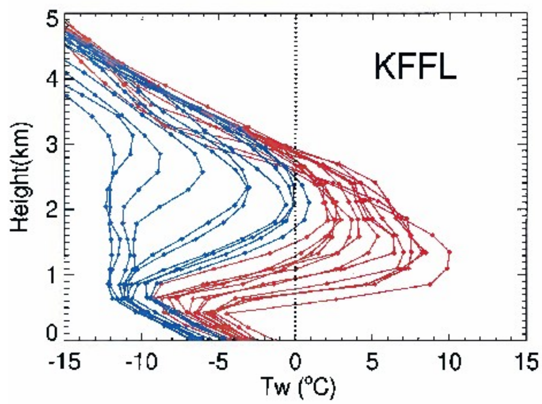

Fig. 2: Vertical profiles of wet bulb temperature (T_w) at Kessler Farm Field Laboratory (KFFL), located at an azimuth of 191.3° and range of 28.5 km from the KOUN radar. Profiles were constructed using RUC model data. Red depicts profiles from 00 to 13 UTC while blue depicts profiles from 14 to 23 UTC on 30 November 2006.

4. Classification based on thermodynamic information

The first step in the classification procedure is to use thermodynamic information obtained from the RUC model to predict the precipitation type at the surface. Vertical profiles of the wet bulb temperature T_w are first calculated across the model grid using T, T_d, and p. If the surface wet bulb temperature T_{ws} > 3°C, it is assumed that precipitation at the surface at that point can be either rain (RA), heavy rain (HR), or hail (HA). If $T_{ws} < 3°C$, however, the vertical profile of T_w at that point is classified as belonging to one of the four different types shown in Fig. 3. H0, H1, and H2 in Fig. 3 depict the heights of 0°C crossing points for the profiles. The precipitation type at the surface is then determined using the flow chart presented in Fig. 4.

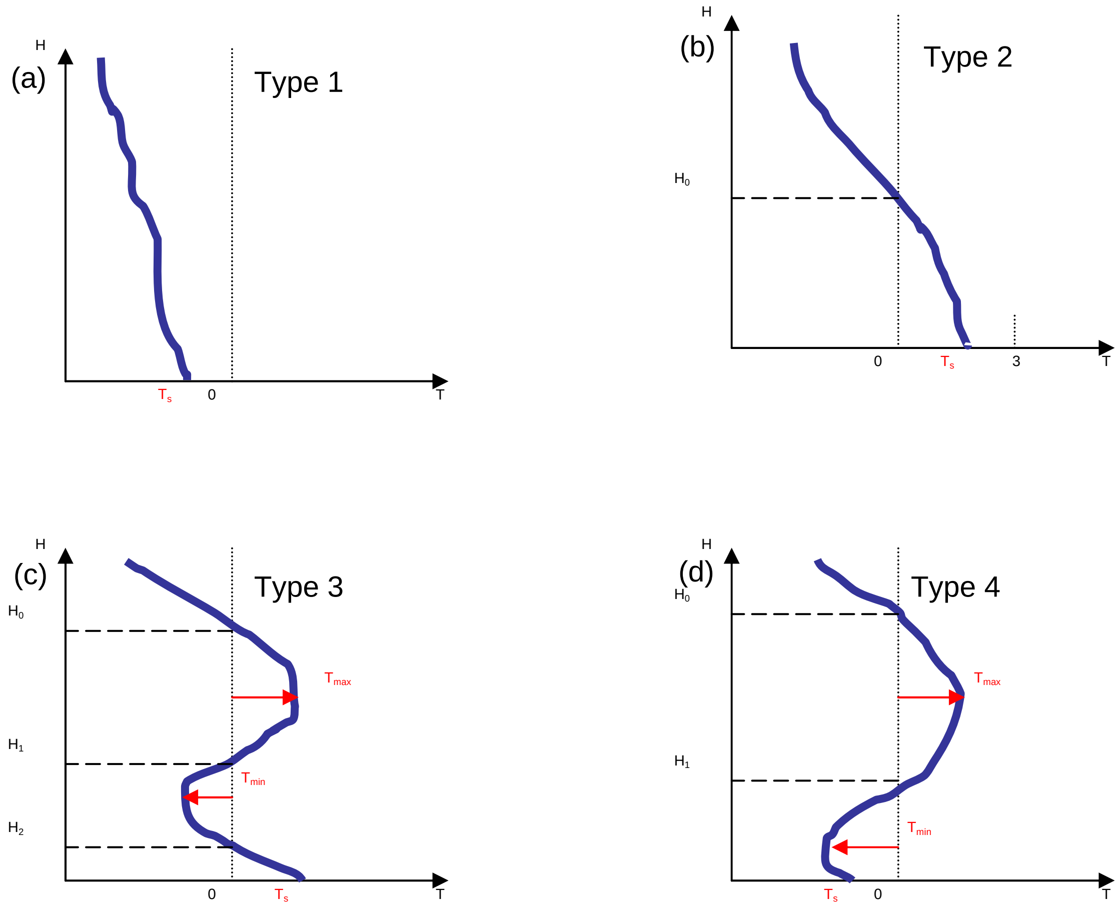

Fig. 3: Four types of vertical profiles of wet bulb temperature (T_w) for which the surface temperature wet bulb temperature (T_{ws}) is less than 3°C.

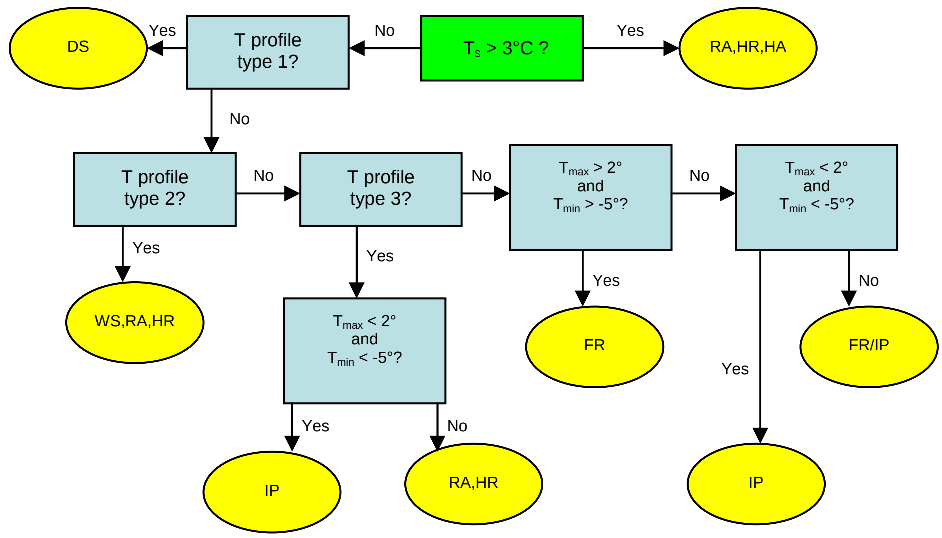

Fig. 4: Flow chart showing logistic for determination of precipitation types depending on vertical profile of wet bulb temperature.

Following Fig. 4, we here describe the procedures for determining precipitation type at the surface. These procedures make use of the studies by Czys et al. (1996), Zerr (1997), and Rauber et al. (2001).

- When $T_{ws} > 3°C$, the precipitation at the surface is classified as either RA, HR, or HA.
- For profile Type 1 (Fig. 4a) where $T_{ws} < 3°C$ and $T_w < 0°C$ throughout the entire depth of the profile, the surface precipitation is classified as DS.
- For profile Type 2 (Fig. 4b), where $T_{ws} < 3°C$ and the T_w profile crosses the 0°C level one time, the precipitation at the surface is classified as WS if $T_{ws} < 3°C$ and H0 < 1 km. Otherwise, the precipitation at the surface is classified as rain (RA) or heavy rain (HR).
- For profile Type 3 (Fig. 4c), where $T_{ws} < 3°C$ and the T_w profile crosses the 0°C level three times, the precipitation at the surface is classified as IP if $0°C < T_{wmax} < 2°C$ and $T_{wmin} < -5°C$, where T_{wmax} is the maximum T_w in the vertical profile and T_{wmin} is the minimum T_w in the vertical profile. Otherwise the precipitation is classified as RA.
- For profile Type 4 (Fig. 4d), where $T_{ws} < 3°C$ and the T_w profile crosses the 0°C level two times, the precipitation at the surface is classified as FR if $T_{wmax} > 2°C$ and $T_{wmin} > -5°C$ and IP if $T_{wmax} < 2°C$ and $T_{wmin} < -5°C$. Otherwise the precipitation at the surface is classified as FR/IP.

Fig. 5 shows the results of this classification scheme, which is based on the profile of T_w determined from the RUC model output over the 24 hour time period from 00 UTC through 23 UTC on 30 November 2006. Radar data from the KOUN radar have been used in Fig. 5 only to assure that the model-based precipitation type classifications are plotted at locations where radar echoes were being observed. In Fig. 5, light blue depicts SN, dark blue WS, green FR, yellow IP, gold FR/IP, and red RA. As depicted in Fig. 5, the classification scheme indicates that precipitation in central Oklahoma started as a mixture of FR/IP on 30 November 2006, with a broad area of RA extending to the south and southeast. Over the next few hours, precipitation in central Oklahoma is shown to quickly transition to IP as the broad region of RA, and a growing intervening belt of FR, pushed off to the southeast. By approximately 18 UTC, precipitation across the entire domain is shown to have transitioned over to SN. These results, serve as a background classification. In the following section, we will demonstrate how polarimetric data from the KOUN radar can be used to modify, or fine tune, this background classification. We will then compare the final precipitation classification against observations.

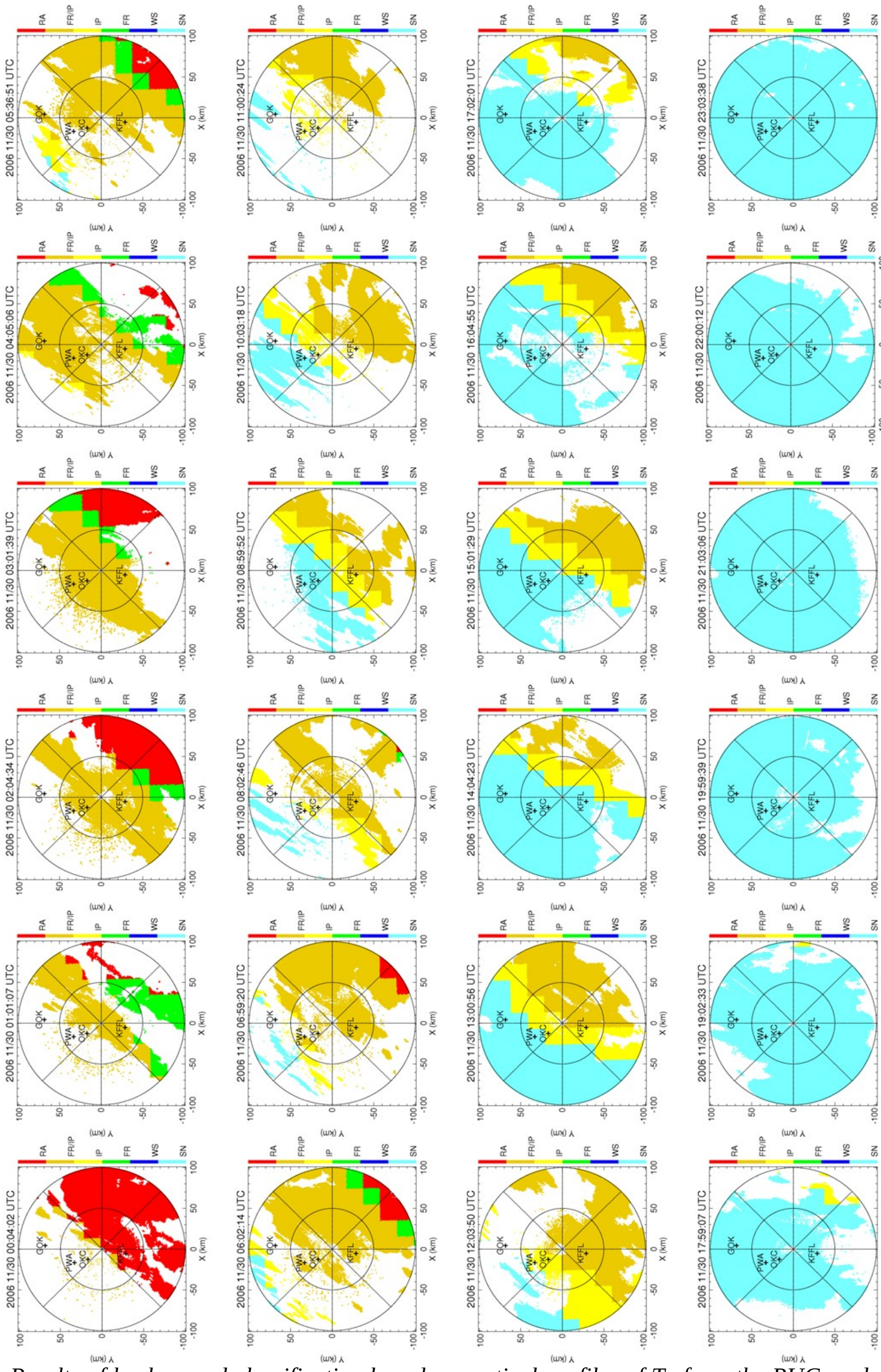

Fig. 5: Results of background classification based on vertical profiles of T_w from the RUC model from 00 UTC through 23 UTC on 30 November 2006. Light blue depicts snow (SN), dark blue wet snow (WS), green freezing rain (FR), yellow ice pellets (IP), gold a combination of freezing rain and ice pellets (FR/IP), and red rain (RA).

5. Polarimetric radar observations

After a preliminary "background" classification of precipitation type is made based on meteorological information, radar data are utilized to (1) determine the location of echoes, (2) confirm or reject the results of the background classification, and (3) to make a distinction between different classes in situations where the background classification does not give definitive answer. For example, discrimination between rain, heavy rain, and hail for $T_s > 3°$ can be done only by combining thermodynamic and radar information. Such a distinction is made using fuzzy logic principles.

Fig. 6 shows an example of a 0.5° elevation PPI from the KOUN polarimetric radar at 0536 UTC on 30 November 2006, along with a corresponding panel depicting the background classification. These data/classifications correspond to the last panel in the top row of Fig. 5 and it can be seen that the radar data has been used to modify the classification results to only plot the background classification where radar echo was observed. At this time, much of the precipitation over central Oklahoma is classified as being either FR or IP. Some information regarding the accuracy of the background classification might be gained from a simple examination of the polarimetric signatures. For example, despite having a Z maximum of only 35 dBZ, the precipitation core to the southeast of the KOUN radar has a $Z_{DR} > 2$ dB over a somewhat broad area, suggesting that the precipitation may indeed be FR rather than IP. To the northwest of KOUN, where Z_{DR} is much smaller, IP is more likely.

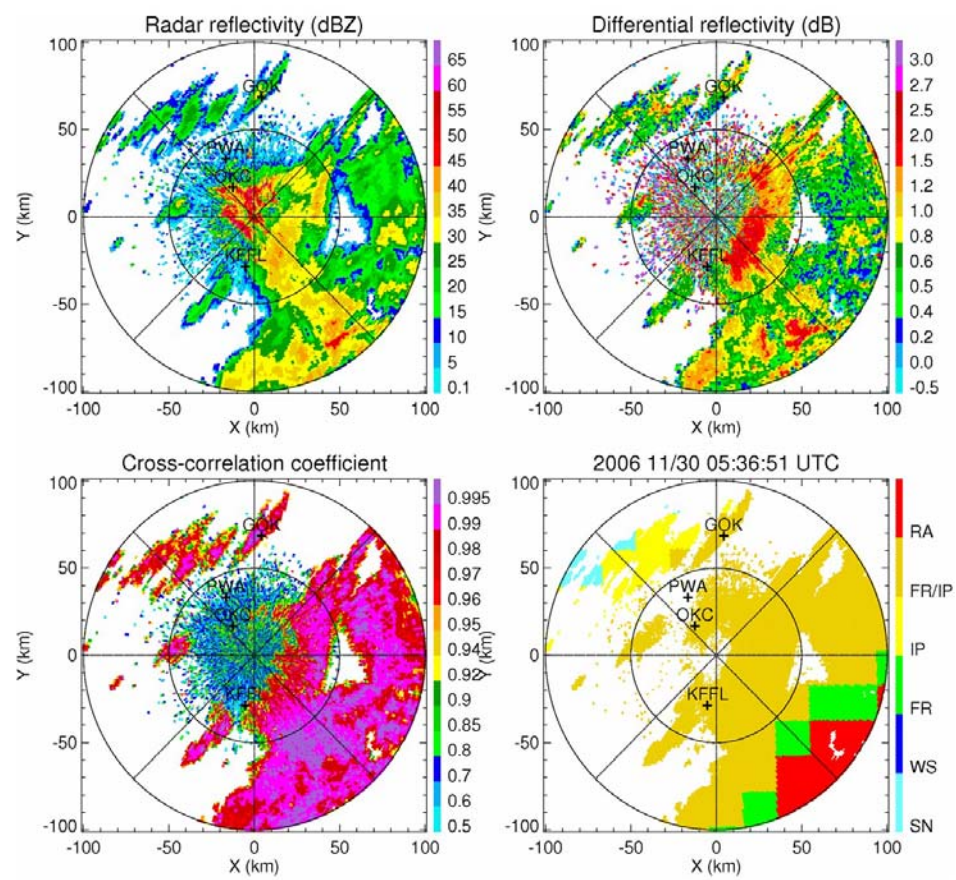

Fig. 6: PPI of KOUN Z, Z_{DR}, and ρ_{HV} at 0.5° elevation, along with results of background classification for 0536 UTC on 30 November 2006. The locations of GOK, PWA, and OKC, which represent sites from which surface data are available to validate the algorithm results (see Fig. 11), are depicted by a '+' in each of the 4 panels.

At the moment, we recommend a conservative approach regarding the use of polarimetric information. This means that the radar is trusted more than thermodynamic information only if polarimetric radar signature is well pronounced and reliable. Polarimetric signatures of the melting layer and hail are examples of such easily recognized and reliable signatures. For example, if the background classifier identifies precipitation at the surface as dry snow (DS) but the radar shows well defined bright band signature aloft, then the background class designation (i.e., DS) should be amended because dry snow at the surface is inconsistent with elevated melting layer. An example of how polarimetric information from aloft can be used to confirm or reject background classification results is shown by Figs. 7 and 8, which present vertical profiles of KOUN Z, Z_{DR}, and ρ_{HV} along a line that passes through OKC (see Fig. 5 for location of OKC with respect to the KOUN radar) at 0327 UTC and 1404 UTC, respectively. On each plot, vertical profiles of T_w from the RUC model are overlaid. The lower right panel of each plot also depicts the locations where polarimetric data indicated a radar bright band signature following the criteria set forth by Giangrande et al. (2008).

We first examine Fig. 7. At this time, the precipitation type recorded at OKC (location indicated by the arrow at approximately -20 km in Figs. 7 and 8) consisted of a mixture of FR and IP. The overlaid T_w contours on Fig. 7 indicate that T_w = -5°C at approximately 3.2 km AGL and T_w = 0°C was at approximately 2.8 km AGL at OKC. Below that level, a deep layer with T_w > 3°C capped another level of T_w = 0°C at 0.7 km AGL. T_w at the surface was approximately -5°C. As would be expected from such a deep layer of warm (T_w > 3°C) air aloft, the radar variables all exhibited characteristics typical of a radar bright band, with a large Z, large Z_{DR}, and low ρ_{HV}. The radar locations that met the bright band detection criteria of Giangrande et al. (2008) are depicted by the pixels (black dots) on the lower right hand panel. The radar determination of a bright band corresponds well with the model indication of an elevated warm layer. The radar data supports precipitation melting aloft and it appears that the background classification of FR and IP at the surface in OKC is warranted.

For contrast, we examine the vertical profile of KOUN data presented in Fig. 8. Here, the model data suggests that the T_w profile above OKC never exceeds 0°C. That is, the warm layer with T_w > 0°C (extending from the right hand side of the figure) is seen to get no closer than 40 km from OKC, which is consistent with the precipitation type observed at OKC. Radar data, however, clearly indicate the presence of a radar bright band. Because of this, it would be necessary to modify the background classification at the surface to exclude the presence of IP.

At present, we follow the criteria presented in Table 1 for the modification of the background classification based on the radar determination of an elevated warm layer.

Based on the above discussion and the criteria presented in Table 1, we present Figs. 9 and 10, which depict the background classification presented in Fig. 5, but with the radar-determined locations of a bright band indicated by the overlaid pixels (Fig. 9) and the background classification corrected (Fig. 10).

Table 1: Criteria used for the modification of the background classification based on the radar determination of an elevated warm layer/bright band.

Elevated warm layer	yes	yes	yes	yes	yes	yes
Background class	SN		All class except for RA	IP	FR/IP	RA
Condition	T_{wmin}< -7 °C	T_{wmin}>-7 °C	Median BBH < 1km			
Surface ID (final)	IP	FR/IP	WS	IP	FR/IP	RA

Elevated warm layer	No		No	No	No	No	No
Background class	SN		IP	FR/IP	RA	FR	WS
Condition	Z_{DR}>0.6 and Z<20 dBZ	otherwise					
Surface ID (final)	CR	DS	IP	FR/IP	RA	FR	WS

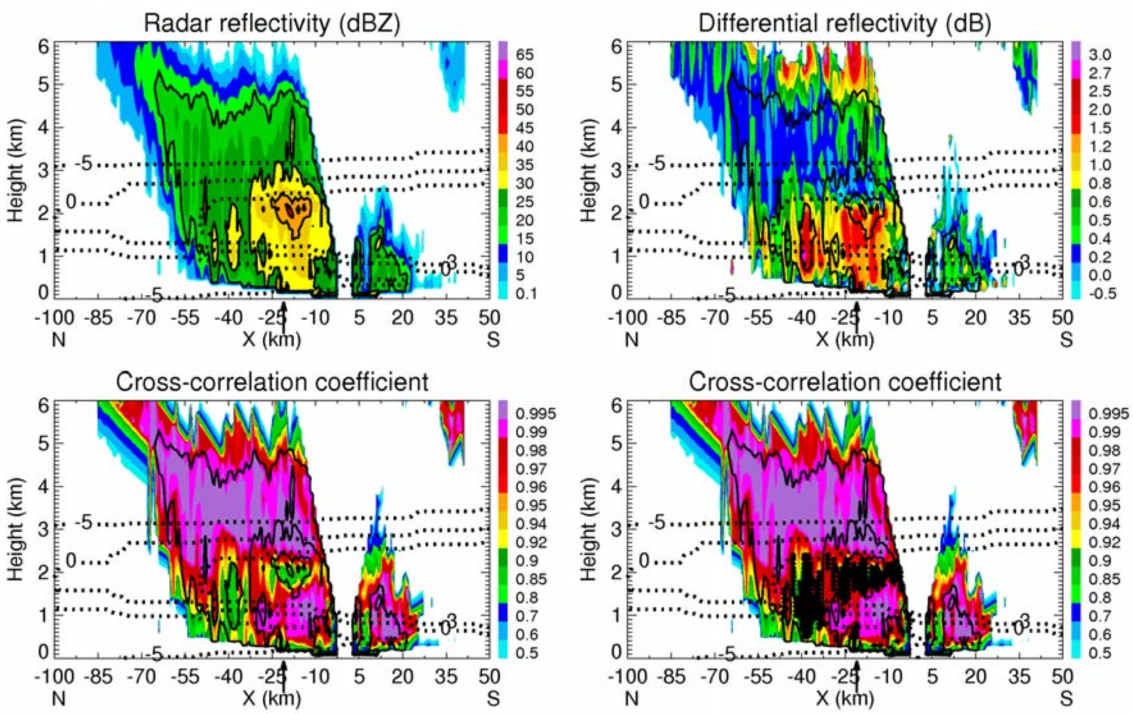

Fig. 7: RHI of KOUN Z, Z_{DR}, and ρ_{HV} at 0327 UTC on 30 November 2006. Overlaid T_w contours are from the RUC model. Melting layer pixels (black dots) overlaid on correlation coefficient on lower right panel indicate locations of radar determined bright band signature.

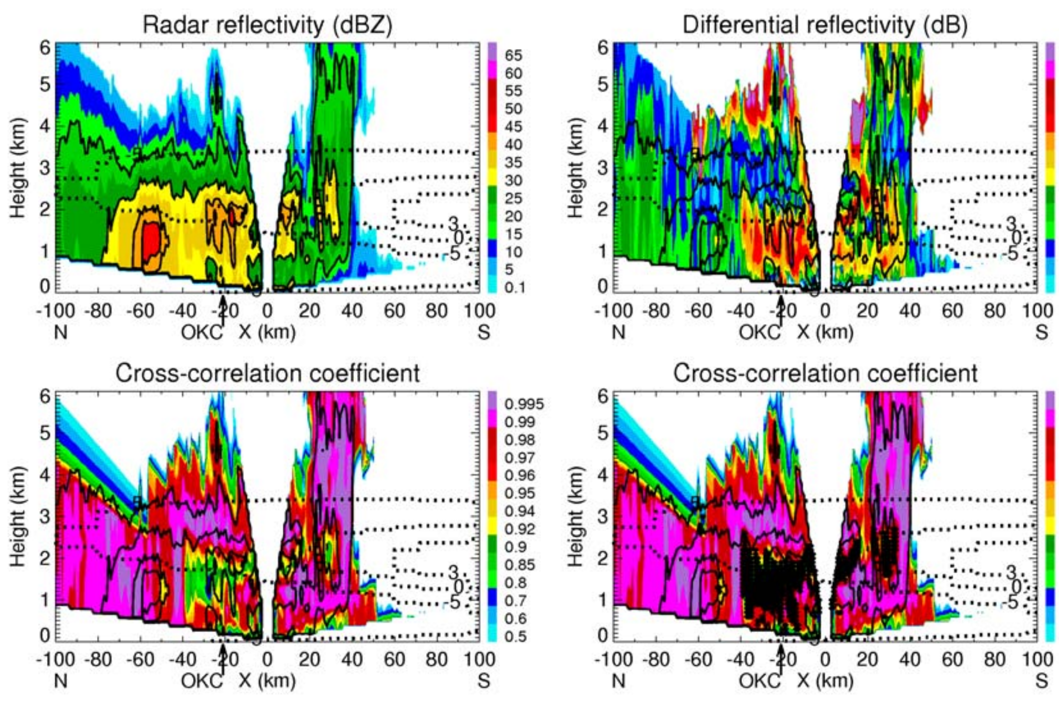

Fig. 8: RHI of KOUN Z, Z_{DR}, and ρ_{HV} at 1404 UTC on 30 November 2006. Overlaid T_w contours are from the RUC model. Melting layer pixels (black dots) overlaid on correlation coefficient on lower right panel indicate locations of radar determined bright band signature.

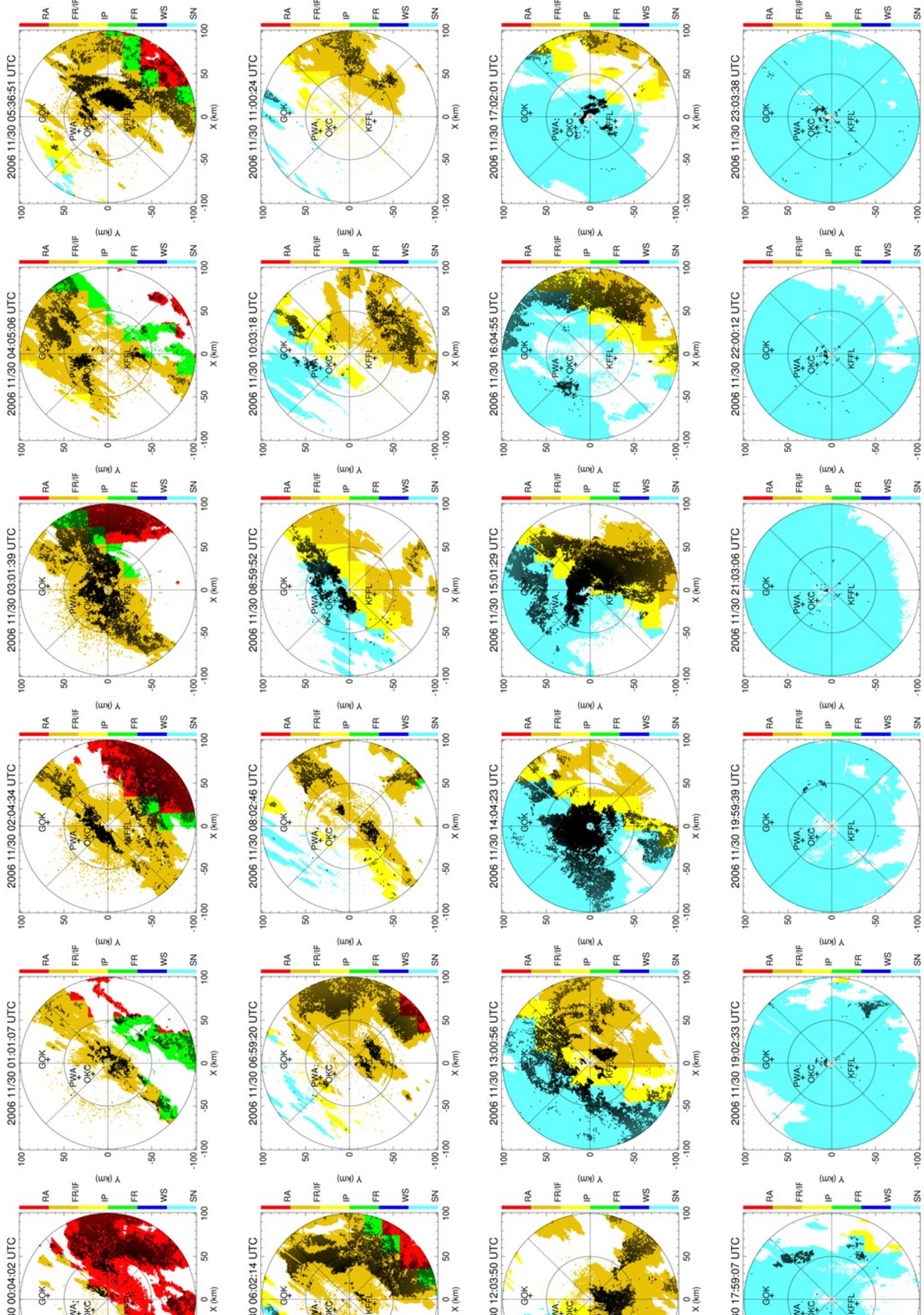

Fig. 9: As in Fig. 5, but with overlaid pixels indicating radar-determined melting layer locations.

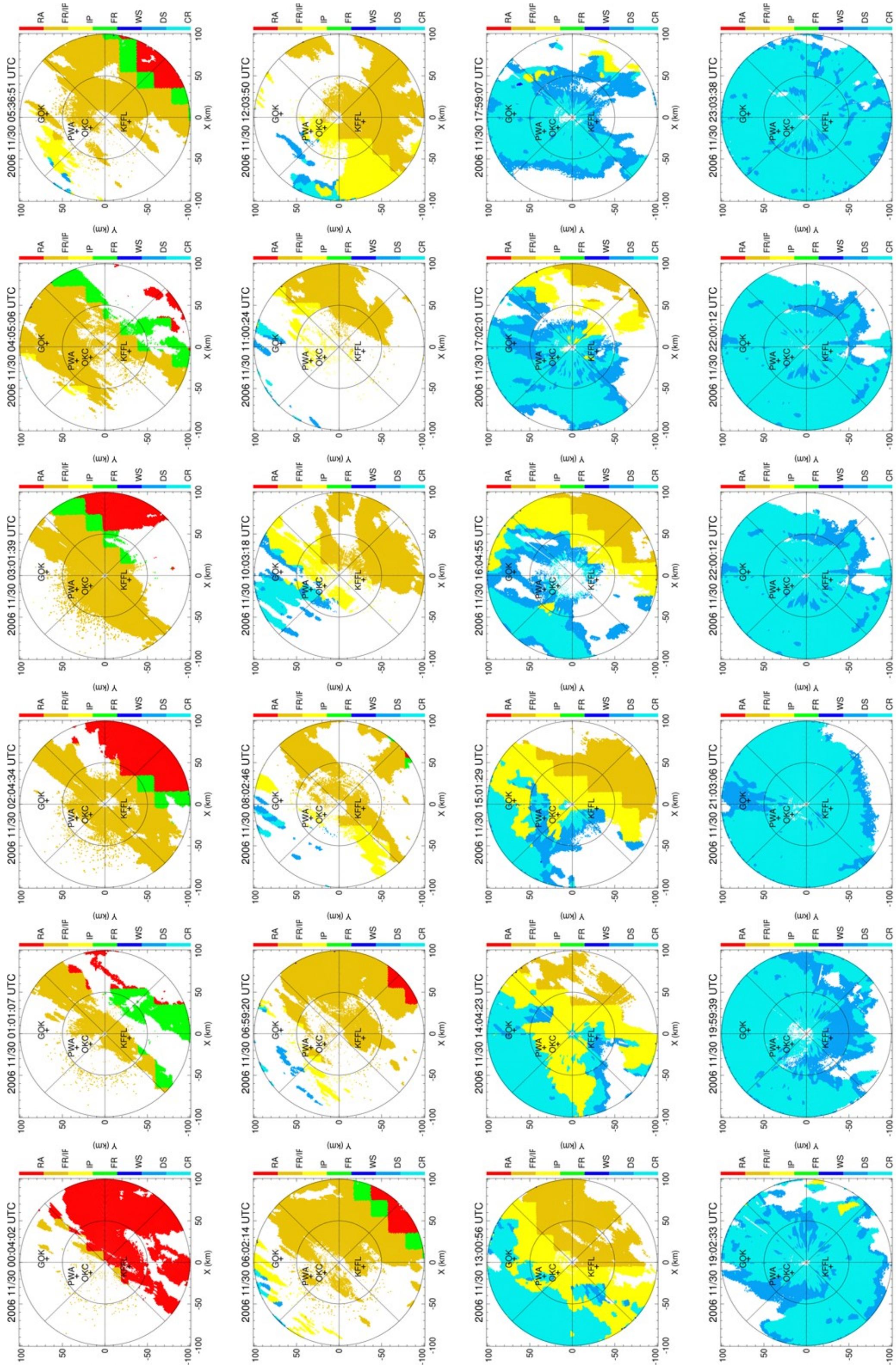

Fig. 10: As in Fig. 9, but with background classification modified.

6. Ground validation

Timelines of observed versus derived precipitation type at GOK, PWA, and OKC (locations are provided in Fig. 5) are shown in Fig. 11. Since the RUC analyses are available only one time per hour, we have assumed that the precipitation type derived by the algorithm is representative of the entire hour following the analysis. The derived precipitation type has reasonable agreement with the observations although there are some obvious discrepancies. Between 0000 and 0600 UTC, the precipitation episodes are rather short-lived and duration appears to be overestimated by the algorithm, particularly at OKC (Fig. 11c). A higher temporal resolution in the model analyses may allow for a better agreement. The precipitation type prior to 1200 UTC is generally well-handled with the algorithm producing either sleet or freezing rain (or a mixed combination of the two) at similar times as in the observations. After 12 UTC, the agreement is rather good at GOK and OKC (Figs. 11a,c, respectively), with the algorithm producing snow at generally the same times as in the observations. There is a slight tendency for the algorithm to produce sleet rather than snow (e.g., between 1300 and 1500 UTC at GOK; Fig. 11a). This may be a result of the algorithm assuming the hydrometeor is generated above the highest freezing level. Cases where the hydrometeors are generated at low levels, below H1 (Fig. 3d), may be incorrectly diagnosed. Problems may also be due to an incorrect estimate of T or T_d by the RUC model. Comparisons of observed and RUC-analyzed T are included in Fig. 11. Notice that the RUC-analyzed T at GOK and PWA is slightly too warm between 1300 and 1500 UTC (Fig. 11a,b, respectively). This time corresponds to a time when the algorithm precipitation type did not agree with the observations. At OKC, the RUC-analyzed T was too cold from 0000 to 1400 UTC and the derived precipitation type did not show as good agreement with the observations. These problems may be addressed with a higher resolution dataset.

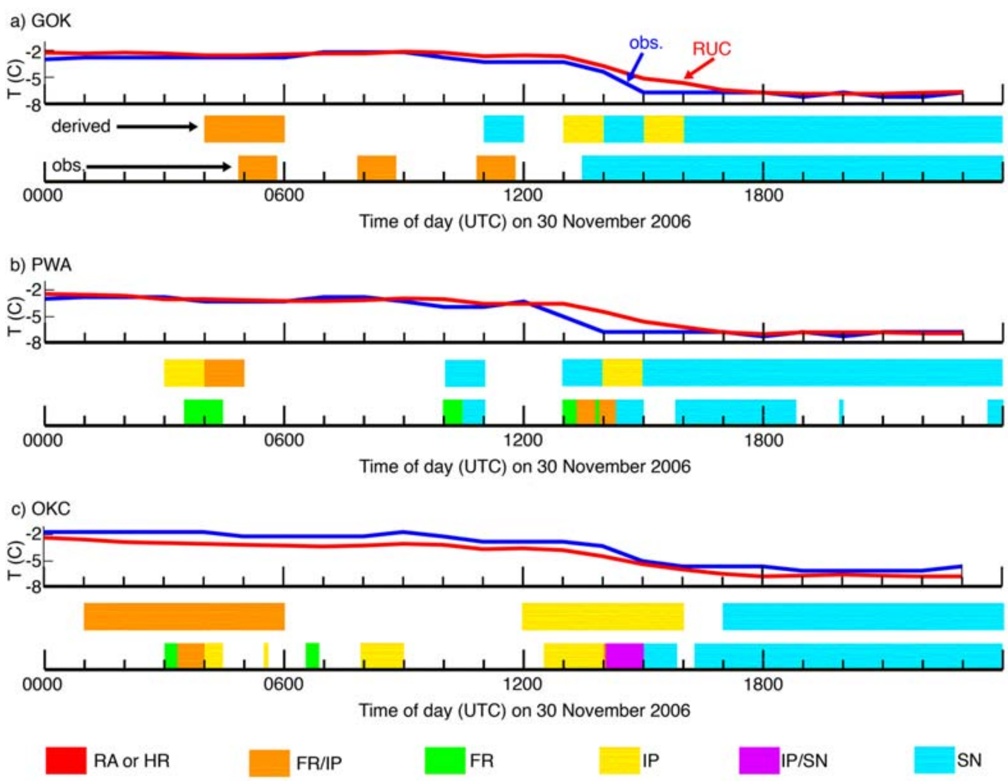

Fig. 11: Top panels: The observed (blue) and RUC-analyzed (red) 2-m temperature. Bottom panels: the derived (top row) and observed (bottom row) precipitation type (shaded as in legend).

7. Conclusions

The algorithm presented in this study attempts to improve upon the existing hydrometeor classification algorithm by introducing thermodynamic data from the RUC model to the classification process. Vertical profiles of wet bulb temperature T_w are first constructed from RUC temperature T, dewpoint temperature, T_d, and pressure p. These profiles are then used to determine a surface precipitation type. When T_w is $< 0°C$ through the entire profile, it is generally safe to classify the surface precipitation type as snow. On the other hand, when single or multiple layers of $T_w > 0°C$ exists, a set of criteria on the depth and temperatures of the layers are used to determine the precipitation type at the ground. This "background classification" is then modified, when necessary, using polarimetric radar data. This is primarily accomplished through the radar determination of whether or not a bright band exists at each location above the background classification grid. When a bright band is observed, surface precipitation types from the background classification that could only be the result of a T_w profile where melting did not occur are considered to be erroneous and modified. In that manner, the radar data are used to either confirm or reject the background classification.

Results of the precipitation classification are validated and confirmed with the data recorded by surface ASOS stations. The algorithm performed well and was especially useful in areas where the melting level was below the lowest beam elevation: a location where radar data alone are insufficient to determine precipitation type.

8. References

Czys, R., R. Scott, K. Tang, R. Przybylinski, and M. Sabones, 1996: A physically based, nondimensional parameter for discriminating between locations of freezing rain and sleet. *Wea. Forecasting*, **11**, 591 - 598.

Giangrande, S. E., J. M. Krause, and A. V. Ryzhkov, 2008: Automated designation of the melting layer with a polarimetric prototype of the WSR-88D radar. *J. Appl. Meteor. Climatol.*, **47**, 1354-1364.

Park, H. -S., A. V. Ryzhkov, S. S. Zrnic, and, K.-E. Kim, 2009: The hydrometeor classification algorithm for the polarimetric WSR-88D: Description and application to an MCS. *Weather and Forecasting*, **24**, 730-748.

Rauber, R., L. Olthoff, and M. Ramamurthy, 2001: Further investigation of a physically based, nondimensional parameter for discriminating between locations of freezing rain and ice pellets. *Wea. Forecasting,* **16**, 185 - 191.

Ryzhkov, A. V., T. J. Schuur, D. W. Burgess, S. E. Giangrande, and D. S. Zrnic, 2005: The Joint Polarization Experiment: Polarimetric rainfall estimation and hydrometeor classification. *Bull. Amer. Meteor. Soc*., **86**, 809-824.

Zerr, R., 1997: Freezing rain, an observational and theoretical study. *J. Appl. Meteor*., **36**, 1647-1661.